

See discussions, stats, and author profiles for this publication at: <https://www.researchgate.net/publication/51064099>

Electrophoretic Characterization of Insulin Growth Factor (IGF-1) Functionalized Magnetic Nanoparticles

ARTICLE *in* LANGMUIR · MAY 2011

Impact Factor: 4.46 · DOI: 10.1021/la2009144 · Source: PubMed

CITATIONS

8

READS

52

5 AUTHORS, INCLUDING:



Julian L Viota

University of Granada

29 PUBLICATIONS 469 CITATIONS

SEE PROFILE



Katarzyna Rudzka

University of Granada

7 PUBLICATIONS 53 CITATIONS

SEE PROFILE



Ignacio Torres-Aleman

Cajal Institute

147 PUBLICATIONS 7,636 CITATIONS

SEE PROFILE



Angel V Delgado

University of Granada

225 PUBLICATIONS 4,132 CITATIONS

SEE PROFILE

Electrophoretic Characterization of Insulin Growth Factor (IGF-1) Functionalized Magnetic Nanoparticles

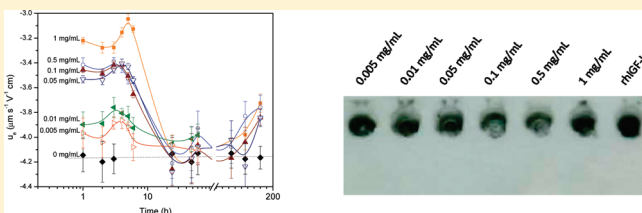
Julián L. Viota,^{*,†} Katarzyna Rudzka,[§] Ángel Trueba,[§] Ignacio Torres-Aleman,[§] and Ángel V. Delgado[‡]

[†]Department of Physics, Campus Las Lagunillas, University of Jaén, 23071, Jaén, Spain

[‡]Department of Applied Physics, School of Science, Campus Fuentenueva, University of Granada, 18071, Granada, Spain

[§]Instituto Cajal, CSIC, and Ciberned, Avd. Doctor Arce 37, 28002, Madrid, Spain

ABSTRACT: The synthesis of composite nanoparticles consisting of a magnetite core coated with a layer of the hormone insulin growth factor 1 (IGF-1) is described. The adsorption of the hormone in the different formulations is first studied by electrophoretic mobility measurements as a function of pH, ionic strength, and time. Because of the permeable character expected for both citrate and IGF-1 coatings surrounding the magnetite cores, an appropriate analysis of their electrophoretic mobility must be addressed. Recent developments of electrokinetic theories for particles covered by soft surface layers have rendered possible the evaluation of the softness degree from raw electrophoretic mobility data. In the present contribution, the data are quantitatively analyzed based on the theoretical model of the electrokinetics of soft particles. As a result, information is obtained on both the thickness and the charge density of the surrounding layer. It is shown that IGF-1 adsorbs onto the surface of citrate-coated magnetite nanoparticles, and adsorption is confirmed by dot-blot analysis. In addition, it is also demonstrated that the external layer of IGF-1 exerts a shielding effect on the surface charge of citrate–magnetite particles, as suggested by the mobility reduction upon contacting the particles with the hormone. Aging effects are demonstrated, providing an electrokinetic fingerprint of changes in adsorbed protein configuration with time.



INTRODUCTION

Nanomedicine is a rapidly growing field and expectations that it will help in improving the treatment of different pathologies are rising high. Metal and semiconductor nanoparticles coupled to biomolecules have recently attracted a great interest because the resulting hybrid materials call for new applications in biological systems.¹ Among such materials, those based on iron oxide nanoparticles are particularly attractive. Because of their magnetic properties, they can be used as magnetic resonance imaging agents in diagnostic protocols, as heat mediators in hyperthermia treatments, and additionally for magnetic guidance in drug delivery applications.

In this scenario, surface functionalization of magnetic nanoparticles is essential for biomedical applications, as that procedure allows targeting against diseased areas or interacting selectively with cells or biomolecules.¹ The binding between magnetite nanoparticles and biomolecules,² achieved by self-assembly of molecules onto the particle surface³ or by methods like the layer-by-layer technique^{4–6} for the deposition of highly charged polyelectrolytes in an organized manner onto charged surfaces, opens new interesting paths to be studied.

In particular, the treatment of many neurodegenerative disorders or brain tumors requires the delivery of specified amounts of drugs to the brain. However, this is hindered by the blood–brain barrier (BBB): this is both a physical barrier and a transport mechanism associated with endothelial cells of the brain capillaries, and it controls the passage of substances from the

blood into the brain and the central nervous system. Therefore, a major challenge for the treatment of brain disorders is to overcome the impediment of therapeutic drugs for entering the brain in sufficient amount.⁷

In the present study we describe the synthesis and characterization of surface functionalized magnetite nanoparticles, with the aim of developing a drug delivery system capable of crossing the blood–brain barrier. We show how electrophoretic mobility measurements allow the characterization of the functionalized nanoparticles serving as a template for the deposition of insulin growth factor 1 (IGF-1). This is a 70-residue single-chain protein that mediates somatic growth and tissue remodeling. It consists of a single polypeptide chain with four domains, which are defined by homology within the insulin-related superfamily.⁸ Despite the similarities of their respective domain regions, insulin and IGF-1 appear to differ in how they bind to their cognate receptors.^{9,10} Because of a functional interaction between the insulin and IGF-1 signaling systems in target tissues, IGF-1 is under investigation as a possible treatment for diverse endocrine and neurodegenerative diseases.^{11–13} An essential characteristic of IGF-1 that makes it an attractive candidate for the treatment of brain diseases is the existence of a physiological mechanism of transfer of circulating IGF-1 into the brain.^{14,15} In addition to

Received: March 10, 2011

Revised: April 8, 2011

Published: April 20, 2011

fundamental roles of the IGF-1, in the early development of the nervous system, Sara et al.¹⁶ reported that IGF-1 contributes to the regulation of neuronal survival and metabolism in the adult brain.

Because of the permeability of the surface layer, the use of classical interpretations (i.e., based on the assumption of rigid, impermeable interfaces) of electrokinetic properties applied to these coated particles are of limited applicability in the electrical characterization of the coated particles. In spite of this, electrokinetic techniques, particularly electrophoresis, have often been employed with that aim; for this it is required to consider the degree of penetration of the flow inside the surface layer and its decay as the rigid core is approached, making the definition of the slip plane and in consequence of electrokinetic potential virtually impossible. Instead, treatments based on the notion of soft particle, pioneered by Ohshima,^{17–20} have become really valuable tools for the electrical characterization of soft interfaces. The model has progressively been improved and made more general by Hill and Saville,^{21–23} Duval et al.,^{24,25} and López-García et al.²⁶ The case of concentrated suspensions was dealt with by Ahualli et al.²⁷ Microbial particles (bacteria, viruses) are archetypes of colloids with such soft interface architecture. The usefulness of electrokinetic techniques and soft-particle theories in characterizing this kind of particles has been repeatedly demonstrated: for example, Clements et al.²⁸ investigated the electrodynamics of *Klebsiella pneumoniae*, relating the interaction of each bacterial strain with eukaryotic cells to the surface charge exhibited by the polysaccharide groups. Langlet et al.²⁹ studied the electrophoretic mobility of the bacteriophage MS2 viral particles, demonstrating the role of the permeability of even the bulk RNA region of the virus. Further studies on the role of physicochemical surface properties on bacterial adhesion and film-forming properties^{30,31} and even on the virulence of the infection³² are also worth to be mentioned.

These treatments have also been applied to a variety of systems, including polymer-covered latex particles¹⁸ or red blood cells.³³ In previous works^{7,34–36} we have also applied such procedures to the evaluation of the membrane and surface properties of montmorillonite clay/humic acid and magnetite/poly(acrylic acid) suspensions.

In this work we report on the coating of IGF-1 on magnetite–citrate particles and the characterization of the complexes produced by means of electrophoresis. Consideration will be given to the fact that the coating of both citrate and IGF-1 can be partially permeable, and hence the mathematical description of the electrokinetic response in these systems must be based on the soft particle model.^{17–27}

MATERIALS AND METHODS

Materials. Water used for the preparation of all suspensions and solutions was deionized in a Milli-Q Academic (Millipore, France) water purification system and filtered through 200 nm membranes; its exit conductivity was about 0.05 $\mu\text{S}/\text{cm}$. All chemicals were purchased from Sigma-Aldrich with analytical quality and were not further purified. Insulin growth factor was purchased from Genpharma S.A. (Buenos Aires, Argentina).

Methods. *Preparation of Magnetite Particles.* Magnetite nanoparticles were synthesized according to the coprecipitation method reported by Massart.³⁷ Briefly, it consists of adding at room temperature 40 mL of an aqueous solution 1 mol/L FeCl_3 and 10 mL of a 2 mol/L FeCl_2 in 2 mol/L HCl solution to 500 mL of 0.7 mol/L aqueous

ammonia solution. After the synthesis, the magnetite nanoparticles were magnetically decanted and redispersed in water at natural pH. This process was repeated several times until the conductivity of the supernatant was below 2 $\mu\text{S}/\text{cm}$. All the samples described below were prepared with a 3% mother solution of magnetite. An average hydrodynamic diameter of 14 ± 4 nm was determined by dynamic light scattering (DLS, Nano ZS, Malvern Instruments, UK) with a polydispersity index below 15%.

As a second step of this investigation, magnetite–citrate nanoparticles were prepared. It can be expected that citrate ions adsorbed onto the surface of magnetite can improve the stability of the magnetic colloids. In addition, citrate coating may have a positive effect on the subsequent protein adsorption as well as on the chances of the particle to cross the BBB, as discussed below.

The preparation of the citrate-coated magnetite particles consisted of dropwise addition of 10 mL of the magnetite mother solution into 1 mL sodium citrate tribasic dihydrate solution at the desired molar concentration under vigorous stirring. It is worth to mention that the resulting dispersion of citrate-coated magnetite visually showed a higher stability than the originally mother magnetite suspension. An average hydrodynamic diameter of 21 ± 3 nm was determined by DLS. The polydispersity index was below 17%.

Finally, IGF-1–magnetite and IGF-1–(citrate-coated) magnetite nanoparticles were prepared by adding dropwise 1 mL of magnetite or citrate (0.1 mol/L)-coated magnetite stock solution respectively to 0.5 mL IGF-1 solutions at the indicated concentrations under permanent but moderate vortexing. The pH of both solutions was previously adjusted to 6 (the isoelectric point of IGF-1 is $\text{pH}_{\text{iep}} = 7.5^{38}$). No change in the color of the suspension could be observed; however, it is worth to mention that the stability of the naked magnetite nanoparticles improved significantly when mixed with the IGF-1 hormone.

Electrical Surface Characterization. Electrophoretic mobility (u_e) measurements were performed in a Malvern Zetasizer 2000 apparatus (Malvern Instruments, UK) at 25 °C. At least nine measurements were performed, changing the sample every three determinations; the mobility result given is the average of all individual data, and the standard deviation of each series is taken as the uncertainty of the determinations. All the samples were previously adjusted to the desired pH, and they were left to equilibrate for 24 h before carrying out the measurements.

IGF-1 Determination by Dot-Blot Analysis. Binding of IGF-1 to nanoparticles was determined by dot-blot analysis. Samples of various preparations of nanoparticles coated with IGF-1 were adsorbed onto a nitrocellulose membrane (10 μL), and after blockade of unspecific binding with 5% defatted milk in Tris-saline buffer, membranes were incubated with antihuman IGF-1 (1/1000 final concentration) for 2 h at room temperature and washed three times with Tris-buffer, and immunoreactivity developed with ECL chemiluminescence after incubation with a peroxidase-labeled secondary antibody. Positive control included human recombinant IGF-1 while unspecific immunoreactivity was ruled out for each sample by omission of the primary antibody.

RESULTS AND DISCUSSION

Electrophoresis of IGF-1-Coated Magnetite. The charge of the magnetite particles is strongly dependent on environmental conditions like pH or ionic strength. In order to optimize the preparation conditions and the final surface charge best suited for drug delivery and immune response, both the bare and coated particles were investigated by means of electrophoretic mobility. It is well-known that this electrokinetic technique is a very useful tool for qualitatively determining the coating efficiency.³⁹

The graphs in Figure 1 depict the dependence of the electrophoretic mobility on the pH of the medium for both magnetite and IGF-1-coated magnetite particles. From an electrokinetic

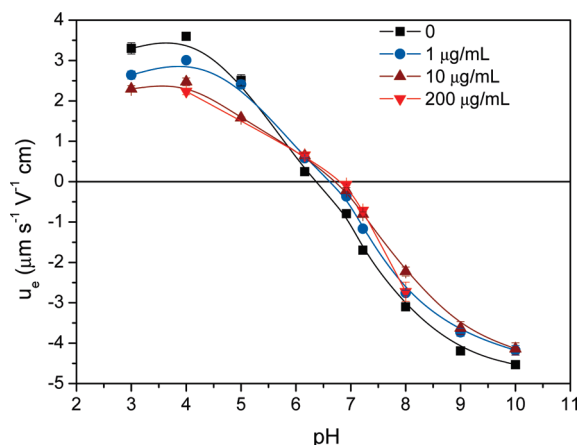


Figure 1. Electrophoretic mobility of magnetite nanoparticles as a function of pH, both bare (data labeled “0”) and after 24 h contact with IGF-1 solutions of the concentrations indicated.

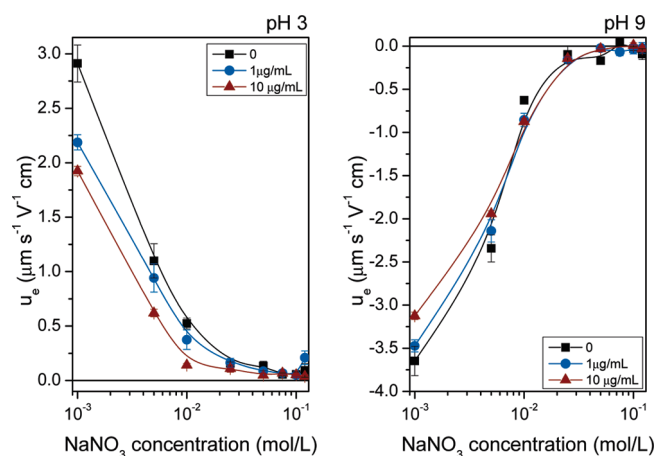


Figure 2. Ionic strength effect on the electrophoretic mobility of magnetite nanoparticles at pH 3 and 9, after 24 h contact with IGF-1 solutions of the concentrations indicated.

point of view, the difference between both kinds of particles can be associated with an adsorption of IGF-1 on the magnetite surface. Magnetite nanoparticles present an isoelectric point in the vicinity of pH 6.5, and the IGF-1 coating produces a drop of $|u_e|$ for all pH values, and this effect is larger the higher the concentration of IGF-1. It is interesting to note that there is a slight shift of the isoelectric point of the IGF-1-coated magnetite particles toward pH 7, whatever the hormone concentration. This shift can be explained by IGF-1 adsorption, considering its above-mentioned isoelectric point at pH 7.5. In addition, the charge inhomogeneity of the protein coating may strongly affect the isoelectric point in dependence of the flow penetration of the liquid in different regions of the protein layer. Such a shift of the isoelectric point is hence a manifestation of the changes in the surface layer thickness when IGF-1 concentration is varied. This was extensively discussed by Langlet et al.,²⁹ both theoretically and by means of electrophoretic mobility measurements in suspensions of the MS2 bacteriophage (Figures 8 and 11 in ref 29, respectively).

We can get a further insight into the solid/liquid interface of these composite systems if we estimate, among other relevant

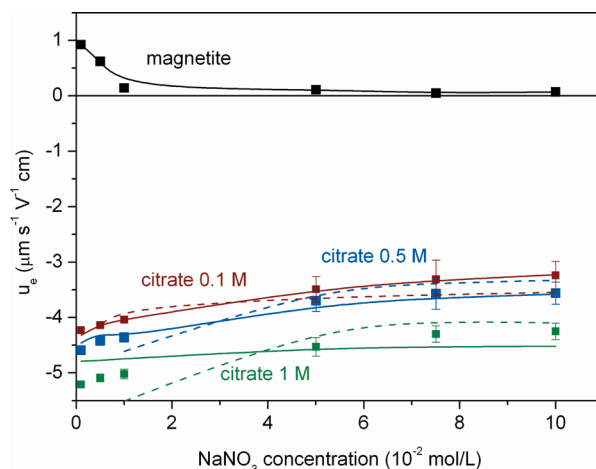


Figure 3. Effect of NaNO_3 molar concentration on the electrophoretic mobility of magnetite particles, both bare and after contact with sodium citrate solutions of the concentration indicated. The dashed lines are best fits to eq 1; solid lines are fits to numerical models^{24,27} (see text).

quantities, the interfacial electric potential. The calculation of the electrokinetic potential (ζ -potential) from mobility data by means of the simple Helmholtz–Smoluchowski or more sophisticated methods, like those by O’Brien and White,⁴⁰ may result in a misleading or even meaningless estimation of ζ for the protein-coated particles. This is because, as noted by Ohshima,^{17–20} electric potential, ionic concentrations, and liquid velocity distribution must be considered, not only in the vicinity of the solid charged surface but also in the soft (liquid penetrable) protein layer. For that reason, our discussion will, for the moment, limit to experimental mobilities. In the Soft-Particles Electrokinetics section we will come back to this issue.

In Figure 2, the electrophoretic mobility of magnetite nanoparticles in the presence of different concentrations of IGF-1 is plotted as a function of NaNO_3 concentration for two pH conditions far from magnetite isoelectric point, i.e., pH 3 and pH 9. As observed, whatever the pH, magnetite nanoparticles show an electrophoretic mobility that tends to zero as the NaNO_3 concentration increases. This behavior, from an electrophoretic point of view, is typical for hard spheres, in spite of the possible presence of IGF-1 on the magnetite nanoparticles. This fact can be associated with a low adsorption of the hormone on the surface of the magnetic carrier. For this reason, an alternative strategy was applied.

Sodium Citrate Coating. Although the interaction of IGF-1 with the magnetic carrier may be Coulombic, hydrophobic, and/or hydrogen bonding, Yamamoto et al.⁴¹ reported that a considerable high concentration of IGF-1 adsorption on acidic gelatin hydrogels was found, due to electrostatic interaction even in solutions of high ionic strength. With this result in mind, and considering the large number of publications reporting high affinity of biomolecules to citrate-gold nanoparticles,⁷ we decided to try surface functionalization of the magnetite cores with sodium citrate prior to adsorption of the IGF-1 hormone. This strategy is further supported by the fact that it was recently found that large amounts of citrate-coated gold nanoparticles (15–50 nm) are able to cross the BBB.⁴² In fact, it has been reported that the negative charge on these systems induces the binding of plasma proteins, such as cationized albumin, which trigger the passage of the BBB and subsequent uptake of particles

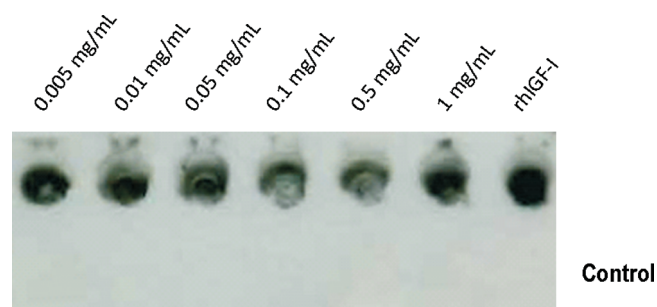


Figure 4. Results of the dot-blot analysis of IGF-1 coupled to citrate-coated ferromagnetic nanoparticles. Recombinant human IGF-1 (rhIGF-1) was used as a positive control, and omission of primary anti-IGF-1 was used for each sample to determine background interference (upper row: results obtained with particles contacted with the IGF-1 concentrations indicated; lower row: control).

by the brain parenchyma.⁴³ Furthermore, the plasma residence time of the particles can be increased by the protein coating, thus increasing their chances to pass the barrier. It is worth mentioning that the BBB, which is composed of a tightly sealed layer of endothelial cells and numerous astrocytes (that regulate the passage and diffusion of the substances), does not allow the access of (i) large molecules (if it is not via receptor-mediated transcytosis) as well as (ii) highly charged and (iii) hydrophilic molecules.^{44,45} Therefore, it is necessary to study, first, if the citrate groups are able to adsorb on the magnetic carriers, second, if the IGF-1 shows evidence of interacting with the citrate groups, and, third, which is the optimal concentration of IGF-1 that best suits the requirements concerning the final charge.

Figure 3 shows the dependence of the electrophoretic mobility with NaNO_3 concentration for both naked and citrate-coated magnetite nanoparticles for three different concentrations (0.1, 0.5, and 1 M) of sodium citrate. From the differences found, it is safe to conclude that citrate molecules adsorb onto the surface of the magnetite nanoparticles. In addition, the citrate-coated magnetite nanoparticles show a negative u_e for all NaNO_3 molar concentration. In all cases the higher the sodium citrate concentration the more negative the mobility.

Dot-Blot Analysis. Figure 4 shows the results corresponding to the dot-blot analysis. This confirmed the presence of immunoreactive human IGF-1 on the nanoparticles. While no dose response was detected, probably due to the amounts of IGF-1 present in the nanoparticle preparation saturating the antibody, specific IGF-1 immunoreactivity was found in all samples of nanoparticles assayed.

Interpretation Based on Soft Particle Electrokinetics. It is worth to note that, contrary to the bare magnetite particles, citrate-coated ones show an electrophoretic mobility practically independent of ionic strength, above 10^{-2} M concentration of NaNO_3 (Figure 3). This kind of behavior is typical of soft particles,^{17–20} as mentioned above. Hence, a study was undertaken of the surface electrical properties of the composite citrate–magnetite and IGF-1–citrate–magnetite particles. Ohshima's approach assumes that the electrical double layer around a solid surface with adsorbed polymer or polyelectrolyte can be separated into two regions: a hydrogel layer of thickness d which contains the adsorbed polyelectrolyte molecules and a diffuse double layer (like the one typically present in rigid particles) roughly starting at the limit of the polymer layer. It is assumed that Donnan equilibrium is established between the two layers

because of the different salt concentrations inside the hydrogel layer and in the surrounding solution. Two electric potentials are thus involved in the overall description of the electrical double layer: the Donnan potential (ψ_{DON}) inside the hydrogel layer and the surface potential (ψ_0) at the boundary between that layer and the bulk solution. The model assumes that the polyelectrolyte segments can be regarded as resistance centers, exerting frictional forces given by $-\gamma \mathbf{u}$ (γ , friction coefficient; \mathbf{u} , liquid velocity inside the polyelectrolyte layer) on the liquid in the hydrogel layer. Considering this additional frictional force in the Navier–Stokes equation inside the hydrogel layer, an expression can be derived that relates the surface potential ψ_0 and the electrophoretic mobility u_e . It is assumed that ionized groups of charge Ze of the polyelectrolyte molecule are uniformly distributed over the polymer layer with a number density N (m^{-3}) and that the liquid contains a symmetrical electrolyte of valence z and bulk concentration n (m^{-3}). More recently, Duval and Ohshima²⁴ analyzed, on the basis of the formalism already proposed by Ohshima, the impact of the characteristic length and interfacial gradients associated with the polymer segment distribution on the electrophoretic behavior of the particle as a whole. Their numerical model applies to arbitrary values of the particle charge, particle radius a , double-layer thickness, and for any charge density profile of the membrane. These authors demonstrated that an approximate analytical expression for the mobility for sufficiently high ionic strengths and arbitrary λd , is given by

$$u_e = \frac{ZeN}{\eta \lambda^2} \frac{\cosh(\lambda d) - 1}{\cosh(\lambda d)} + \frac{\varepsilon}{\eta} \frac{\psi_0 / \kappa_m + \psi_{\text{DON}} / \lambda}{1 / \kappa_m + 1 / \lambda} \quad (1)$$

where ε is the electric permittivity of the liquid medium, η is its viscosity, λ is a dimensionless frictional parameter given by $(\gamma / \eta)^{1/2}$, and κ_m is the effective Debye–Hückel parameter of the surface hydrogel layer, involving the contribution of the fixed charge ZeN . The parameter $1/\lambda$ can be considered to characterize the softness of the polyelectrolyte layer, and it is a measure of the flow penetration distance inside the polyelectrolyte membrane. The corresponding expressions for ψ_{DON} , ψ_0 , and κ_m are given by^{17,20}

$$\begin{aligned} \psi_{\text{DON}} &= \frac{kT}{ze} \sinh^{-1} \left(\frac{ZN}{2zn} \right) \\ \psi_0 &= \psi_{\text{DON}} - \frac{kT}{ze} \tanh \left(\frac{Ze\psi_{\text{DON}}}{2kT} \right) \\ \kappa_m &= \kappa \left[\cosh \left(\frac{ze\psi_{\text{DON}}}{kT} \right) \right]^{1/2} \end{aligned} \quad (2)$$

where k is Boltzmann's constant, e is the electron charge, T is the absolute temperature, and κ is the Debye–Hückel parameter of the solution. It must be noted that eq 1 is valid if the electric double layer is thin in comparison with both the particle radius and the membrane thickness.

Briefly, the method followed involves fitting eq 1 to the experimental data of the electrophoretic mobility of core/shell particles as a function of electrolyte concentration. A least-squares procedure allows obtaining the best-fit parameters, d , ZN , and λ , for the model chosen, since the core size was independently obtained from TEM and DLS measurements.

For the experiments, the electrophoretic mobility was measured immediately after the particles were mixed in solutions with different salt concentrations. The results obtained using this

Table 1. Best-Fit Parameters of the Mobility Data in Figure 3 to the Duval–Ohshima Model^{24 a}

citrate concn (M)	<i>d</i> (nm)	λa	Magnetite–Citrate			
			ZN (mmol/L)	ψ_{DON} (mV)	ψ_0 (mV)	κ_m^{-1} (nm)
0.1	5	0.5	−70.6	−46.8	−28.2	2.89
0.5	11	0.7	−71.8	−48.6	−29.6	2.89
1.0	14	0.6	−77.6	−53.1	−33.2	3.93

IGF-1 concn (mg/mL)	<i>d</i> (nm)	λa	Magnetite–0.1 M Citrate–IGF-1			
			ZN (mmol/L)	ψ_{DON} (mV)	ψ_0 (mV)	κ_m^{-1} (nm)
0.01	16	0.5	−56.6	−45.3	−27.2	2.89
0.5	23	0.5	−71.6	−43.6	−25.8	2.89

^a *d* = layer thickness, λa = softness parameter, ZN = layer charge density, ψ_{DON} = Donnan potential, ψ_0 = surface potential, and κ_m^{-1} = effective double layer thickness.

Table 2. Best-Fit Parameters of the Mobility Data in Figure 3 to the Duval–Ohshima Numerical Model^{24,27 a}

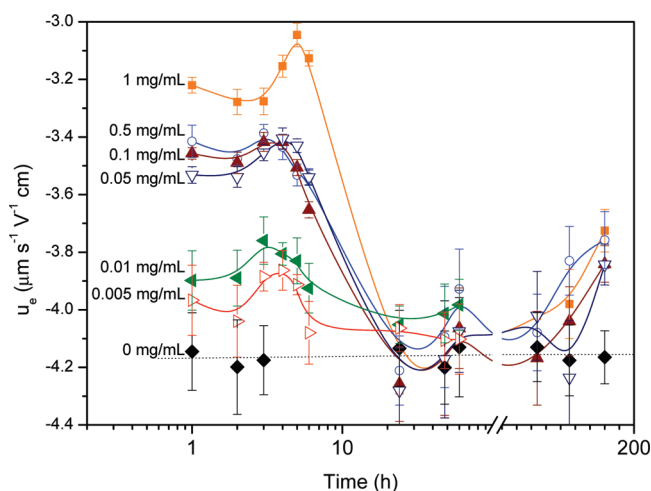
citrate concn (M)	<i>d</i> (nm)	λa	Q_{citrate} (10^{-17} C)	ZN (mmol/L)
0.1	2.5	0.3	−7.1	−88.5
0.5	3.3	0.5	−6.8	−61.3
1.0	6.0	0.5	−5.7	−28.7

^a *d* = layer thickness, λa = softness parameter, Q_{citrate} = total layer charge, and ZN = layer charge density.

procedure are displayed in Figure 3 (dashed lines), which shows the expected electrophoretic nonzero mobility plateau for the highest ionic strengths. This plateau is an evidence of the presence of a soft, hydrodynamically permeable layer that surrounds the particle.¹⁷ It must be recalled that, as depicted in Figure 2, the electrophoretic mobility of rigid particles at high ionic strength should go to zero because of the so-called double-layer compression, i.e., the reduction of the potential at the electrokinetic plane (the zeta potential) because of the screening of the surface charge by the large amounts of counterions in the double layer.

The dashed lines in the Figure show how the model nicely fits the experimental data in the high salt concentration range. The iterative least-squares fitting procedure yielded the *d*, ZN, and λ values included in Table 1 for the three sodium citrate concentrations. From the best-fit parameters, the effective Debye–Hückel thickness (κ_m^{-1}), the Donnan potential (ψ_{DON}), and the surface potential (ψ_0) can be calculated using eq 2. The results from these calculations are also reported in Table 1. The deviations of the fits from the experimental data, found at the low ionic strength regime, are expected considering the validity of eq 1, restricted to high ionic strengths. In addition, it is worth to mention that these deviations can be related to double-layer polarization effects and/or to heterogeneity in surface layer distribution following heterogeneous expansion of layer as a result of swelling processes, as reported by Duval et al.²⁵

For these reasons, we also used a more complete model, in which concentration polarization of the double layers is included and where no limitations have to be applied to the parameter values. This generalization of the theory of soft-particle electrokinetics was elaborated, as above-mentioned, in refs 24 and 26 and extended to arbitrary volume fraction of solids in ref 27. For this work, the numerical treatment described by Ahualli et al.²⁷ was employed. The fitting procedure involved again a least-squares

**Figure 5.** Electrophoretic mobility of magnetite–citrate–IGF-1 nanocomposites as a function of time, for different concentrations of IGF-1 in solution. Citrate concentration: 0.1 mol/L, pH 7.4.

method, and the fitted parameters were *d*, λ , and the layer charge (Q_{citrate} and from this the density of charged groups ZN). As above, the size and the charge (actually the electrokinetic charge) of the cores are known from independent determinations. The best-fit theoretical (solid) lines are included in Figure 3, and Table 2 displays the values of the fitted parameters. Note that the agreement with the experimental data is largely improved, as expected, considering that the small particle radius of the magnetite cores prevents the fulfilling of the condition $\kappa a \gg 1$, except at very high ionic strength. The full theory indicates that contacting the particles with increasing concentrations of sodium citrate gives rise to a thicker coating, but not necessarily a more highly charged one. It is suggested that the citrate ions will not tend to form multilayers on the particles, due to electrostatic repulsion, but rather we can picture the process as the formation of more extended coatings the larger the citrate concentration, as citrate ions compete for adsorption sites on the surface of the cores. Nevertheless, it is worth mentioning that, in spite of the approximations involved in eq 1, the fitted parameters are very similar in both the approximate analytical expression and the numerical method. This reinforces the physical significance of the Ohshima–Duval approach for the electrokinetics of soft particles.

Plotted in Figure 5 are the experimentally determined electrophoretic mobilities of IGF-1–citrate–magnetite complexes at pH 7.4 as a function of time, for six IGF-1 concentrations (0.005–1 mg/mL) and for a citrate concentration of 0.1 mol/L. As observed, u_e is negative no matter the concentration of IGF-1 present in the solution. At the initial time (when the citrate-coated magnetite nanoparticles are just mixed with the IGF-1 solution), comparison between IGF-1-coated and uncoated particles suggests that the hormone has a screening effect on the surface charge associated with the adsorbed citrate. In fact, for all samples it was found that the higher the concentration of IGF-1, the higher is the screening of the charge, and therefore the smaller is the electrophoretic mobility of the samples. With the aim of estimating the surface potential of the composite IGF-1–citrate–magnetite nanoparticles, the analytical model (eq 1) was applied to two of the IGF-1-coated samples (IGF-1 concentrations: 0.01 and 0.5 mg/mL). The results of the best fits are presented in Table 1. As can be seen, our qualitative arguments are confirmed, and the higher the IGF-1 concentration, the smaller the Donnan and surface potentials obtained for the composite particles. Note also that the layer expands (d increases) upon rising the hormone concentration, an additional sign of protein coating.

Aging Effects. Finally, with the aim of studying the process of IGF-1 adsorption on the surface of citrate–magnetite particles, the electrophoretic mobility of the composite particles was studied as a function of time (Figure 5). As observed, it was found that for all samples u_e reaches a maximum between the third and the sixth hour after mixing the magnetite–citrate composites with the IGF-1 solutions. This maximum can be easily associated with an increased deposition/adsorption of IGF-1 molecules on the surface of the citrate-coated nanoparticles. In addition, it is also worth to mention that a few hours after this maximum the mobility increases in absolute values and a sort of plateau is reached. This plateau in u_e can be associated with a possible structural relaxation/desorption of the IGF-1 molecule at the surface of the magnetite–citrate particles. According to Norde,⁴⁶ once the protein molecule has attached, it relaxes toward its equilibrium structure. Furthermore, relaxation is retarded as the protein molecule has a strong internal coherence, and it requires optimization of protein/surface interactions, and a certain degree of “spreading” of the protein molecule over the sorbent surface, developing a larger number of protein–surface contacts. Phenomenologically, a system is in equilibrium if no changes take place at constant surroundings. It seems that this equilibrium is reached after ~ 200 h. Note that after that time the value of u_e for the IGF-1-coated citrate–magnetite nanoparticles is very similar whatever the initial IGF-1 concentration within a certain range of values for u_e (3.7 – $3.8 \mu\text{mV}^{-1} \text{s}^{-1} \text{cm}$). In all cases the presence of IGF-1 on the surface can be confirmed from the difference between the long-time mobility plateau and the u_e value obtained in the absence of hormone contact ($u_e \approx -4.2 \mu\text{mV}^{-1} \text{s}^{-1} \text{cm}$) (Figures 3 and 5).

CONCLUSIONS

We have described the characterization of surface-functionalized magnetite prepared with the aim of developing magnetic drug delivery vehicles capable of surpassing the blood–brain barrier and releasing their load of the insulin growth factor (IGF-1). To that aim, the magnetic nuclei were coated successively with sodium citrate and the IGF-1 hormone. All coating steps with

sodium citrate and IGF-1 were followed by electrophoretic mobility measurements. The adsorption of the hormone manifests in a clear decrease of the absolute value of the electrophoretic mobility. In addition, the dot-blot analysis confirmed the presence of immunoreactive human IGF-1 on the nanoparticles.

The presence of the hormone provides a soft coating on the rigid core particles. This is demonstrated by the fact that the electrophoretic mobility does not tend to zero at high ionic strengths, so that a deformable layer can be identified which avoids the surface charge screening by ions in solution. A theoretical model accounting for the existence of such charged layer is used for the estimation of the friction parameter and Donnan potential of the adsorbed hormone coating. Interestingly, electrokinetic techniques such as electrophoresis can also be used to detect aging effects associated with conformation changes in the adsorbed hormone. These results appear as a very promising connection between electrokinetic characterization and design of nanoparticle-based drug vehicles.

AUTHOR INFORMATION

Corresponding Author

*E-mail: jlvota@ujaen.es; phone +34 953 212425; fax +34 953 212838.

ACKNOWLEDGMENT

Financial support by Ministerio de Ciencia e Innovación (Projects FIS2010-19493 and SAF 2009-06367-E), FEDER funds, and Junta de Andalucía (Project PE-2008 FQM 3993) of Spain, is gratefully acknowledged. J.L.-V. was supported by MICINN, Spain, under the “Juan de la Cierva” programme. The valuable assistance of Dr. S. Ahualli in the numerical resolution of soft-particle electrokinetic equations is also acknowledged.

REFERENCES

- (1) Taton, T. A.; Mirkin, C. A.; Letsinger, R. L. *Science* **2000**, *289*, 1757–1760.
- (2) Viota, J. L.; Arroyo, F. J.; Delgado, A. V.; Horno, J. J. *Colloid Interface Sci.* **2010**, *344*, 144–149.
- (3) Ulman, A. *Chem. Rev.* **1996**, *96*, 1533–1554.
- (4) Decher, G. *Science* **1997**, *277*, 1232–1237.
- (5) Möhwald, H. *Colloids Surf., A* **2000**, *171*, 25–31.
- (6) Chanana, M.; Gliozzi, A.; Diaspro, A.; Chodnevskaja, I.; Huewel, S.; Moskalenko, V.; Ulrichs, K.; Galla, H. J.; Krol, S. *Nano Lett.* **2005**, *5*, 2605–2612.
- (7) Viota, J. L.; Mandal, S.; Delgado, A. V.; Toca-Herrera, J. L.; Möller, M.; Zanuttin, F.; Balestrino, M.; Krol, S. *J. Colloid Interface Sci.* **2009**, *332*, 215–223.
- (8) Blundell, T. L.; Humbel, R. E. *Nature* **1980**, *287*, 781–787.
- (9) de Meyts, P.; Whittaker, J. *Nat. Rev. Drug Discovery* **2002**, *1*, 769–783.
- (10) Whittaker, J.; Groth, A. V.; Mynarcik, D. C.; Pluzek, L.; Gadsboll, V. L.; Whittaker, L. J.; Whittaker, J. *J. Biol. Chem.* **2001**, *276*, 43980–43986.
- (11) Pennisi, P.; Gavrilova, O.; Setser-Portas, J.; Jou, W.; Santopietro, S.; Clemmons, D.; Yakar, S.; LeRoith, D. *Endocrinology* **2006**, *147*, 2619–2630.
- (12) Watanabe, T.; Miyazaki, A.; Katagiri, T.; Yamamoto, H.; Idei, T.; Iguchi, T. *J. Am. Geriatr. Soc.* **2005**, *53*, 1748–1753.
- (13) Aleman, A.; Torres-Aleman, I. *Prog. Neurobiol.* **2009**, *89*, 256–265.
- (14) Carro, E.; Nunez, A.; Busiguina, S.; Torres-Aleman, I. *J. Neurosci.* **2000**, *20*, 2926–2933.

- (15) Nishijima, T.; Piriz, J.; Duflot, S.; Fernandez, A. M.; Gaitan, G.; Gomez-Pinedo, U.; Garcia Verdugo, J. M.; Leroy, F.; Soya, H.; Nuñez, A.; Torres-Aleman, I. *Neuron* **2010**, *67*, 834–846.
- (16) Sara, V. R.; Clayton, K.; Cooke, P.; Craven, C. J.; Garcia-Aragon, J.; Harmon, B.; Harvey, M.; Haase, H.; Plenderleith, M.; Richardson, N.; Sherrard, R.; Stahlbom, P.-A.; Walker, G.; Walsh, T. P. *Dev. Brain Disfunct.* **1996**, *9*, 85–92.
- (17) Ohshima, H. In *Interfacial Electrokinetics and Electrophoresis*; Delgado, A. V., Ed.; Marcel Dekker: New York, 2002; pp 123–146.
- (18) Ohshima, H.; Makino, K.; Kato, T.; Fujimoto, K.; Kondo, T.; Kawaguchi, H. *J. Colloid Interface Sci.* **1993**, *159*, 512–514.
- (19) Ohshima, H. *Colloids Surf., A* **1995**, *103*, 249–255.
- (20) Ohshima, H. In *Electrical Phenomena at Interfaces: Fundamentals, Measurements, and Applications*; Ohshima, H., Furusawa, K., Eds.; Marcel Dekker: New York, 1998; pp 19–55.
- (21) Hill, R. J.; Saville, D. A. *Colloids Surf., A* **2005**, *267*, 31–49.
- (22) Hill, R. J.; Saville, D. A.; Russel, W. B. *J. Colloid Interface Sci.* **2003**, *258*, 56–74.
- (23) Hill, R. J. *Phys. Rev. E* **2004**, *70*, 051406.
- (24) Duval, J. F. L.; Ohshima, H. *Langmuir* **2006**, *22*, 3533–3546.
- (25) Duval, J. F. L.; Gaboriaud, F. *Curr. Opin. Colloid Interface Sci.* **2010**, *15*, 184–195.
- (26) Lopez-Garcia, J. J.; Grosse, C.; Horno, J. J. *Colloid Interface Sci.* **2003**, *265*, 327–340.
- (27) Ahualli, S.; Jiménez, M. L.; Carrique, F.; Delgado, A. V. *Langmuir* **2009**, *25*, 1986–1997.
- (28) Clement, A.; Gaboriaud, F.; Duval, J. F. L.; Farn, J. L.; Jenney, A. W.; Lithgow, T.; Wijburg, O. L. C.; Hartland, E. L.; Strugnell, R. A. *PLoS One* **2008**, *3*, e3817.
- (29) Langlet, F.; Gaboriaud, F.; Gantzer, C.; Duval, J. F. L. *Biophys. J.* **2008**, *94*, 3293–3312.
- (30) Dague, E.; Duval, J. F. L.; Jorand, F.; Thomas, F.; Gaboriaud, F. *Biophys. J.* **2006**, *90*, 2612–2621.
- (31) Duval, J. F. L.; Buscher, H. J.; van de Belt-Gritter, B.; van der Mei, H. C.; Norde, W. *Langmuir* **2005**, *21*, 11268–11282.
- (32) Gosselin, F.; Duval, J. F. L.; Simonet, J.; Ginevra, C.; Gaboriaud, F.; Jarraud, S.; Mathieu, L. *Colloids Surf., B* **2011**, *82*, 283–290.
- (33) Hyono, A.; Gaboriaud, F.; Mazda, T.; Takata, Y.; Ohshima, H.; Duval, J. K. L. *Langmuir* **2009**, *25*, 10873–10885.
- (34) Ramos-Tejada, M. M.; Ontiveros, A.; Viota, J. L.; Duran, J. D. G. *J. Colloid Interface Sci.* **2003**, *268*, 85–95.
- (35) Viota, J. L.; de Vicente, J.; Duran, J. D. G.; Delgado, A. V. *J. Colloid Interface Sci.* **2005**, *284*, 527–541.
- (36) Viota, J. L.; de Vicente, J.; Ramos-Tejada, M. M.; Durán, J. D. G. *Rheol. Acta* **2004**, *43*, 645–656.
- (37) Massart, R. *IEEE Trans. Magn.* **1981**, *17*, 1247–1248.
- (38) Holland, T. A.; Tabata, Y.; Mikos, A. G. *J. Controlled Release* **2005**, *101*, 111–125.
- (39) Goodman, C. M.; McCusker, C. D.; Yilmaz, T.; Rotello, V. M. *Bioconjugate Chem.* **2004**, *15*, 897–900.
- (40) O'Brien, R. W.; White, L. R. *J. Chem. Soc., Faraday Trans.* **1978**, *274*, 1607–1626.
- (41) Yamamoto, M.; Ikada, Y.; Tabata, Y. *J. Biomater. Sci. Polym.* **2001**, *12*, 77–88.
- (42) Sonavane, G.; Tomoda, K.; Makino, K. *Colloids Surf., B* **2008**, *66*, 274–280.
- (43) Sousa, F.; Mandal, S.; Garrovo, C.; Astolfo, A.; Bonifacio, A.; Latawiec, D.; Menk, R. H.; Arfelli, F.; Huewel, S.; Legname, G.; Galla, H.-J.; Krol, S. *Nanoscale* **2010**, 2826–2834.
- (44) Rubin, L. L.; Staddon, J. M. *Annu. Rev. Neurosci.* **1999**, *22*, 11–28.
- (45) Spencer, B. J.; Verma, I. M. *Proc. Natl. Acad. Sci. U.S.A.* **2007**, *104*, 7594–7599.
- (46) Norde, W. In *Physical Chemistry of Biological Interfaces*; Baszkin, A., Norde, W., Eds.; Marcel Dekker: New York, 2000; p 121.